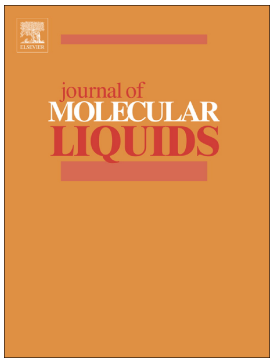

Synthesis, characterization, and determination of critical micellar concentration and thermotropic phase transition of taurolipids

Sengan Megarajan, Pothiappan Vairaprakash, Veerappan Anbazhagan

PII: S0167-7322(16)33981-2
DOI: doi: 10.1016/j.molliq.2017.03.064
Reference: MOLLIQ 7099

To appear in: *Journal of Molecular Liquids*

Received date: 10 December 2016
Revised date: 16 March 2017
Accepted date: 17 March 2017

Please cite this article as: Sengan Megarajan, Pothiappan Vairaprakash, Veerappan Anbazhagan , Synthesis, characterization, and determination of critical micellar concentration and thermotropic phase transition of taurolipids. The address for the corresponding author was captured as affiliation for all authors. Please check if appropriate. Molliq(2017), doi: 10.1016/j.molliq.2017.03.064

Revised version – correction marked

Synthesis, characterization, and determination of critical micellar concentration and thermotropic phase transition of taurolipids

Sengan Megarajan, Pothiappan Vairaprakash, Veerappan Anbazhagan*

Department of Chemistry, School of Chemical and Biotechnology, SASTRA University, Thanjavur – 605043, Tamil Nadu, India

*Corresponding author,

V. A: Phone: +91 4362-264101-3689; Fax: +91 4362-264120,,

e-mail: anbazhagan@scbt.sastra.edu

Abstract

Taurolipids (NAT) are a newer class of fatty acid amides (FAA) identified in the central nervous system, liver, and kidney of fatty acid amide hydrolase knockout mice. In this study, we reported a convenient method to synthesize NATs in fair yield and characterized using FTIR, ^{1}H-NMR and ^{13}C-NMR. Fluorescence spectroscopy study showed that NATs form micelles in an aqueous environment and the critical micellar concentration (CMC) follows a linear trend with respect to fatty acid acyl chain length. Differential scanning calorimetry reveals that NATs undergoes broad endothermic transition with transition temperatures increases with increasing fatty acid acyl chain length though the magnitude of change from one chain length to another chain length decreases as the acyl chain length increase. The transition enthalpy (ΔH_t) and transition entropy (ΔS_t) corresponding to the chain-melting phase transition depends linearly on the acyl chain length and fitted to a linear equation, which yielded the incremental values, ΔH_{inc} (1.09 ± 0.03 kcal.mol^{-1}) and ΔS_{inc} (2.96 ± 0.16 cal.mol^{-1}.K^{-1}), contributed by each methylene unit to ΔH_t and ΔS_t. The end contributions arising from the head group and the terminal methyl group were calculated to be ΔH^0 = -7.28 ± 0.46 kcal.mol^{-1} and ΔS^0 = -17.36 ± 2.11 cal.mol^{-1}.K^{-1}. Thermodynamic parameters, incremental values of ΔH_{inc} and ΔS_{inc} suggest that the acyl chains in NATs are tightly packed and the obtained larger negative ΔS^0 suggest that the hydration of polar sulfonate group of NATs also play an important role in the self-assembly of NATs.

Keywords: N-acyltaurine; taurolipids; critical micellar concentration; phase transition; fluorescence; differential scanning calorimetry

1. Introduction

Fatty acid amides (FAA) are well known as an endogenous signaling molecule and possess numerous physiological functions in mammalian tissues [1]. For example, anandamide (arachidonoyl ethanolamide) is an endogenous cannabinoid neurotransmitter [2], oleoylethanolamide regulates appetite through the activation of G-protein coupled receptor [3], erucamide ($22:1^{13}$) is the major angiogenic component stimulates new blood vessel formation [4], arachidonoylglycine does not bind to the cannabinoid receptors, but relieves pain [5], virodhamine relaxes arteries through endothelial cannabinoid receptors [6]. The advent of mass spectrometry facilitated the field of lipidomics and identified newer fatty acid amide signaling molecules in mammalian tissues, but their site of action is largely unknown [7]. Moreover, isolation of FAA from the tissues is largely complicated because these classes of lipids are often synthesized, released and inactivated proximal to their sites of action [1]. In order to investigate the biology of newly identified FAA, researchers required a reasonable quantity of FAA. This will be possible through developing devoted synthetic strategy and physicochemical characterization of FAA.

Fatty acids that are amidated to taurine are collectively known as *N*-acyltaurines or taurolipids (NAT) [8]. NAT was first identified in the central nervous system (CNS), liver and kidney of fatty acid amide hydrolase (FAAH) knockout mice [8]. NAT isolated in the liver and kidney were predominantly polyunsaturated compounds (~160 pmol/g in kidney; ~20 pmol/g in liver), while long chain saturated and monounsaturated *N*-acyl chains were the most common in CNS (upto 2 nmol/g) [9]. The enzymes, the acyl-CoA: amino acid *N*-acyltransferase (ACNAT1) [10] and the bile acid-CoA: amino acid *N*-acyltransferase (BAT) [11] have been proposed for the production of *N*-acyltaurines. Long et al., study suggested the existence of a transport system for NAT that transfers these lipids from liver to other tissues [12]. It has been noted that the endogenous levels of NAT were elevated following acute or chronic inactivation of FAAH, suggests that NAT could form a major signaling system similar to other FAA [13]. *N*-arachidonyltaurine activates several transient receptor potential (TRP) channels, including TRPV1 and TRPV4 calcium channels, both of which are expressed in the kidney [13]. TRP channels are suggested to playing a role in the regulation of osmotic

sensation and blood pressure. Treatment with *N*-arachidonyltaurine and *N*-oleoyltaurine showed a marked reduction in the proliferation of prostate cancer PC-3 cells [14]. NAT regulates insulin secretion from pancreatic β-cells through TRPV1 channels and other receptor channels also involved in the insulin secretion response to treatment with NAT [15]. The biology of NAT remains elusive, even though studies with mouse tissues shown their presence with diverse *N*-acyl chain length in plasma, heart, brown and white adipose tissue, lung, kidney, testis, liver and spleen [12].

While compared to other FAAs like *N*-acyl ethanolamine [16, 17], *N*-acyl aminoacids [18, 19, 20], *N*-acyl dopamine [21], there are no reports on the physicochemical characterization of NAT. As a first step in learning about NAT, we are reporting a facile method to synthesise *N*-acyltaurine with saturated acyl chains of even number of carbon atoms and studied their thermotropic phase behaviour using differential scanning calorimetry (DSC) and determined the critical micellar concentration (CMC) of NAT using fluorescence probes. The CMC of NAT was found to decrease with increase in the acyl chain length. DSC study showed that the transition enthalpies and entropies of hydrated NATs exhibit a linear dependence on the acyl chain length. Most of the phase transition occurred over a broad temperature range, suggesting that NAT undergoes a phase transition from the micellar to the monomeric state.

2. Material and methods

2.1. Materials

Decanoylcholoride (N10), laurylchloride (N12), myristoylchloride (N14), palmitoylchloride (N16), stearoylchloride (N18), taurine (T), 8-anilinonapthalene sulfonic acid (ANS) and *N*-phenylnapthalamine (NPN) were obtained from Sigma, India. All other reagents were of reagent grade and were obtained from local suppliers. Solvents were distilled and dried prior to usage.

2.2. Synthesis of N-acyltaurines

N-acyltaurines are synthesized in fair yield by a condensation reaction between taurine and fatty acid chloride. In a typical synthesis, taurine (275 mg, 2.2 mmol) (i) was mixed with sodium hydroxide (395 mg, 9.8 mmol) and hydrated with 500 μL of water and then added tetrahydrofuran (10 mL). To the resulting mixture, acid chloride (2 mmol) was added under constant stirring and the reaction was allowed to proceed for 12 h at room temperature. The progress of the reaction was followed by thin-layer chromatography (TLC) on silica gel (solvent system: acetic acid: water: *n*-butanol, 1:1.4:2 v/v) and the TLC plates were stained with ninhydrin (20 mg ninhydrin dissolved in 9.5 mL of *n*-butanol and 0.5 mL of 10% methanol). Noteworthy, taurine showed pink color while staining with ninhydrin whereas *N*-acyltaurines appears in yellow color. After the completion of reaction, the reaction mixture was centrifuged at 3000 rpm for 15 min and the resultant crude *N*-acyltaurine (iii) was subjected to column chromatography. Briefly, the crude NAT was loaded onto silica gel column and washed with 100% ethyl acetate to remove unreacted fatty acids. Further elution with the mixture of solvent containing methanol and ethyl acetate (20:80 v/v) yielded pure *N*-acyltaurines as judged by ^{1}H-NMR and ^{13}C-NMR. The isolated yields of different NATs range from 60-65 %. ^{1}H NMR (300 MHz), ^{13}C NMR (75 MHz) were recorded on Bruker-300-Advance II spectrometer, with D_2O or CD_3OD as solvent and tetramethylsilane (TMS) as reference (δ = 0 ppm). The chemical shifts are expressed in δ downfield from the signal of internal TMS. FT-IR spectra were recorded using a PerkinElmer spectrum by adopting KBr pellet method.

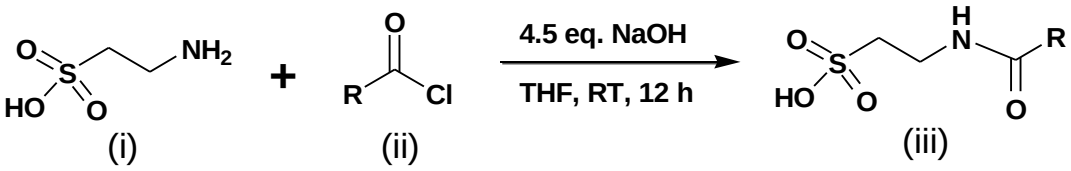

R: CH_3-$(CH_2)_8$; CH_3-$(CH_2)_{10}$; CH_3-$(CH_2)_{12}$; CH_3-$(CH_2)_{14}$; CH_3-$(CH_2)_{16}$

Scheme 1: Synthesis of *N*-acyltaurine from taurine and fatty acid chloride

2.3. Determination of critical micellar concentration

The CMC of NATs was determined by fluorescence spectroscopy using the fluorescent probe, ANS and NPN [22, 23]. Fluorescence measurements were performed on a JASCO spectrofluorometer FP8200 with a 1.0 cm quartz cell. The fluorescence of ANS (10 μM) was recorded between 400-650 nm, keeping the excitation wavelength at 370 nm and the slit widths of both excitation and emission set at 5 nm. The fluorescence of NPN (5 μM) was recorded between 360-600 nm, keeping the excitation wavelength at 340 nm. The stock solution of 100 mM, 80 mM, 15 mM, 5 mM and 1 mM of N10T, N12T, N14T, N16T and N18T, respectively was prepared by dissolving exactly weighed NAT in 10 mM sodiumphosphate buffer, pH -7.4. Briefly, 3 mL of fluorescent probe (ANS or NPN) was titrated by adding small aliquots of NATs from a concentrated stock solution and the fluorescence spectrum was measured after an equilibration period of 2 min. The fluorescence intensity at fixed wavelength was then plotted as a function of NATs concentration and the CMC was determined as the concentration where a distinct break in the slope was observed. Prior to analysis, fluorescence intensities were corrected for volume changes. 10 mM phosphate buffer, pH-7.4 was used throughout the study and experiments were performed at 25^{o}C. All experiments were repeated at least three times to arrive at the average values.

2.4. Differential scanning calorimetry

Samples for DSC was prepared by suspending accurately weighed NATs (5-6 mg) with 10 mM phosphate buffer, pH-7.4. N12T and N14T were hydrated at room temperature, whereas N16T and N18T were hydrated by heating the suspension to ~65^{o}C. The hydrated samples and buffer were loaded into the sample and reference cell, respectively, of a Nano DSC-TA instrument, India. A scan rate of 1^{o}C/min was used. Three heating

scans were performed for each sample and the scans were found to be reproducible. All heating scans were normalized with respect to concentration of NAT, which yields the heat capacity (ΔC_p) in kcal/mol.K. Transition temperature (T_t), transition enthalpy (ΔH_t) for each transition was estimated by integrating the area under the transition using the software provided with the instrument. In all cases, only the first heating scans were considered for further analysis. Transition entropies (ΔS_t) were estimated from the ΔH_t assuming a first order transition according to the expression [24]:

$$\Delta H_t = T_t . \Delta S_t \qquad (1)$$

3. Results and discussion

3.1. Synthesis of N-acyltaurine

Taurine fatty acid conjugates were synthesized by reacting taurine and fatty acid chloride in THF in the presence of NaOH at room temperature for 12 h (Scheme 1). Our initial efforts on pre-activating fatty acid chloride as NHS-ester derivative and reacting with taurine failed to yield the corresponding product. Then, the condensation between taurine and fatty acid chloride was carried out utilizing various organic bases and organic solvent system (Table 1). In chloroform, both inorganic bases and organic bases did not yield the product (Table 1, entries 1 - 4). In acetonitrile solvent, *N*-acyltaurine was obtained in trace quantities using Et_3N as base (Table 1, entry 5). Adding traces of water to the reaction medium improved the yield to 12 % (Table 1, entry 6). Under same condition, using NaOH as base further improved the product formation and the corresponding *N*-acyltaurine was obtained in 27 % (Table 1, entry 7). Using THF/water mixture as solvent and NaOH as base increased the product yield to 62 % (Table 1, entry 8).Though the base NaOH is expected to compete with taurine in the nucleophilic attack in aqueous system, given solvent system [THF/H_2O (19:1, v/v)] reduces the availability of NaOH for nucelophilic attack and we could able to get the product in better yields. Taurolipids were purified by flash chromatography and characterized by TLC, ^{1}H-NMR and ^{13}C-NMR. IR spectra of all NATs showed absorption bands corresponding to the amide I at 1640-1645 cm^{-1} and amide II at 1540-1553 cm^{-1}. The amide N-H stretching was observed at 3337-3284 cm^{-1} and N-H bending was seen at 1552-1540 cm^{-1}. The stretching, bending and rocking modes of the polymethylene group of the hydrophobic acyl chain was observed at 2919-2916 cm^{-1}, 1470-1467 cm^{-1} and 718-721 cm^{-1}, respectively (Fig. S1- S5). The ^{1}H NMR spectra of NAT showed resonances at 3.44 -3.60 δ (2H, t) and 2.98-2.96 δ (2H, t) for the methylene groups at α and β positions to the sulfonate moiety, 2.11-2.19 δ (2H, t) and 1.46-1.61 δ (2H, bs) for the methylene group at α and β positions to the amide carbonyl, respectively. Resonance of the terminal methyl group was seen at 0.92−0.74 δ (3H, t), whereas the resonance of the polymethylene group was observed at 1.16−1.30 δ (12−28H, m). These spectral data are presented in the supporting information. The ^{13}C NMR spectra of NAT showed resonances at 13.70 δ for terminal methyl group of the acyl

chain, 49.9 δ for the methylene moiety at α positions of the sulfonate group, 35.10 δ for the methylene moiety attached to NH and C=O group, other methylene carbons are seen at 29.3, 25.6 and 22.6 δ. Resonance corresponds to the amide carbonyl was observed at 175.9 δ. For all the synthesized compounds, number and nature of ^{1}H NMR resonances are matching with the structure of the corresponding compounds. For compounds N10T and N12T, the numbers of ^{13}C NMR resonances are well in accordance with structure. For the compound N14T, few resonances are grouped into single peak, hence the number of resonances observed are less in number than the expected number. For compounds N16T and N18T, ^{13}C NMR spectra were not recorded due to solubility problem. These spectral data are presented in the supporting information (Fig. S6 to S13).

Table 1. Condensation of taurine with lauroyl acid chloride*

entry	Base	Solvent	Result
1	$NaHCO_3$	Chloroform	No reaction and lauroyl acid was recovered
2	K_2CO_3	Chloroform	
3	Pyridine		
4	Et_3N	Chloroform	
5	Et_3N	CH_3CN	NAT was obtained in trace quantities
6	Et_3N	CH_3CN/H_2O (19:1, v/v)	NAT was obtained in 12% yield
7	NaOH	CH_3CN/H_2O (19:1, v/v)	NAT was obtained in 27% yield
8	NaOH	THF/H_2O (19:1, v/v)	NAT was obtained in 62% yield

*To a mixture of taurine (1.0 mmol) and a base (5 equiv) in specified solvent (5.0 mL), lauoryl chloride (1.0 mmol) was added and stirred for 12 h.

3.2. Determination of critical micellar concentration

An amphiphilic molecule with long acyl chain fatty acids was preferred to adopt one of the following structures in hydrated form: interdigitated gel phase, hexagonal phase and micelles [25, 26]. NAT is composed of a polar sulfonate group and hydrophobic acyl chain, therefore, it is expected that NAT can form micelles in aqueous solution. Fluorophores like 8-anilinonapthalene-1-sulfonate were widely used to determine the critical micellar concentration of an amphiphilic molecule [22]. ANS is weakly fluorescent in aqueous solution and exhibit strong fluorescence in lipophilic environment.

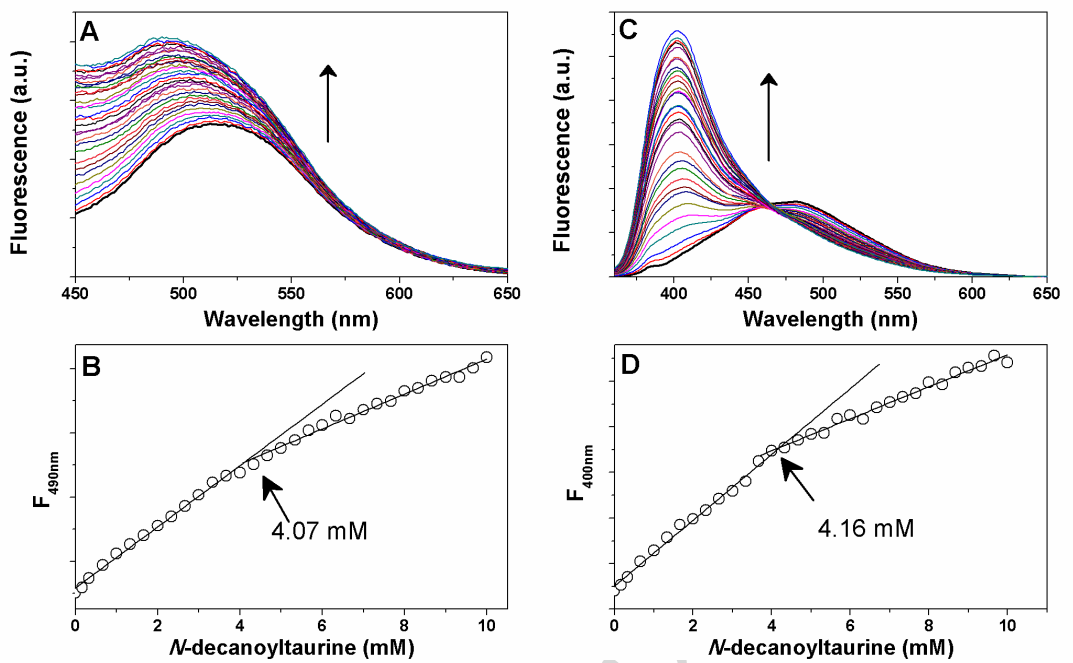

Figure 1: (A) Fluorescence spectra of ANS at various concentration of N10T. (B) Fluorescence intensity of ANS is plotted as a function of N10T concentration. (C) Fluorescence spectra of NPN at various concentration of N10T. (D) Fluorescence intensity of NPN is plotted as a function of N10T concentration. Increasing concentration of a 100 mM stock solution of N10T was added to 3 mL of ANS/NPN. Excitation wavelength for ANS and NPS is 340 nm and 370 nm, respectively. Solutions were prepared in 10 mM phosphate buffer, pH -7.4. Temperature = 25^{o}C.

Fig. 1A shows the effect of *N*-decanoyltaurine (N10T) on the emission spectra of ANS. The addition of N10T increases the emission intensity of ANS and induces a blue shift of about 30 nm in the peak wavelength, indicating that the environment of ANS becomes more hydrophobic. Fig. 1B shows the enhancement of fluorescence intensity at 490 nm as a function of N10T concentration. Two straight lines can be drawn through the experimental points; their intersection (4.07 mM) is taken as the critical micellar concentration (CMC) above which N10T aggregates to form micelles (Fig. 1B). The CMC of N10T was also studied with another fluorescent probe, NPN [23]. Fig. 1C shows that the addition of N10T increases the emission intensity of NPN and a blue shift of about 70 nm in the peak wavelength. The determined CMC (4.16 mM) is comparable to the CMC determined with ANS (Fig. 1D), suggesting that both probes are suitable for the determination of CMC of an amphiphilic molecule. The fluorimetric method of CMC determination was further verified by surface tension measurement. The CMC of N12T

determined by pendant drop method using goniometer is 1.99 mM (Fig. S14). This value is in close agreement with the reported fluorimetric method (Table 2), indicate that ANS and NPN is a suitable probe to study the CMC of NAT. The results of fluorescence titration of ANS with *N*-lauryltaurine (N12T), *N*-myristoyltaurine (N14T), *N*-palmitoyltaurine (N16T) and *N*-stearoyltaurine (N18T) are shown in Fig. 2 and the CMC values are reported in Table 2. Noteworthy that, the addition of 50 mM of sodium chloride prevents the formation of micelles, indicate the contributions of electrostatics in the formation of micelles (Fig. S15).

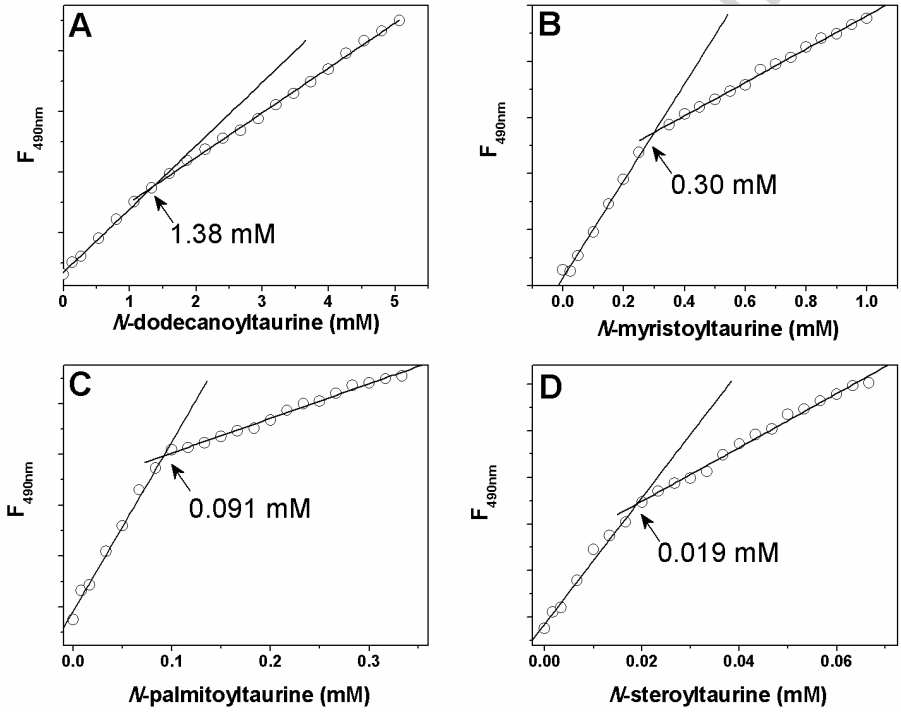

Figure 2: Fluorescence titration of ANS with (A) N12T, (B) N14T, (C) N16T and (D) N18T. The concentration of ANS is 5 μM. 80 mM, 15 mM, 5 mM and 1 mM stock solution of N12T, N14T, N16T and N18T, respectively were used in the titration. Solutions were prepared in 10 mM phosphate buffer, pH -7.4. Temperature = 25^{o}C.

Table 2: Critical micellar concentration of various *N*-acyltaurines. CMC values given are the averages obtained from three independent experiments and reported as mean with standard error.

NAT	CMC determined with the fluorescent probe	
	ANS (mM)	NPN (mM)
N10T	4.005 ± 0.092	3.975 ± 0.262
N12T	1.460 ± 0.113	1.660 ± 0.566
N14T	0.272 ± 0.040	0.305 ± 0.050

N16T	0.082 ± 0.013	0.117 ± 0.037
N18T	0.018 ± 0.001	0.023 ± 0.001

The relationship between the CMC values and the carbon number of the alkyl chain in *N*-acyltaurine is shown in Fig. 3. This plot gave a good linear relationship and followed Traube's rule [27]. The slope of the line yields a value for $\Delta G/RT$ and the energy of micellar formation deduce from the slope is of -0.61 kcal/mol per methylene group of the alkyl chain, which is close to those obtained with lysolecithin [28].

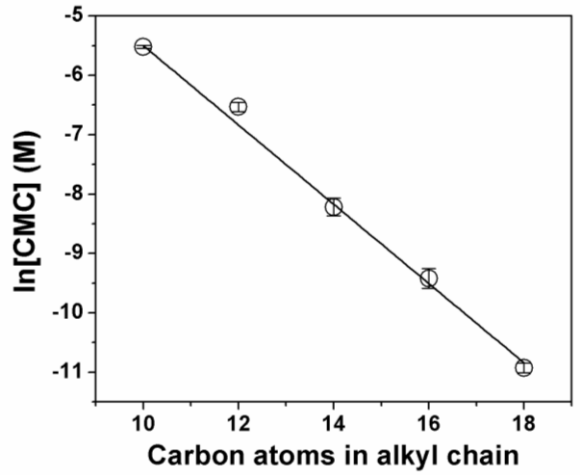

Figure 3: Logarithm of CMC as a function of carbon numbers of the alkyl chain in *N*-acyltaurine. Some data point's error bar is smaller.

3.3. Phase transitions of NAT

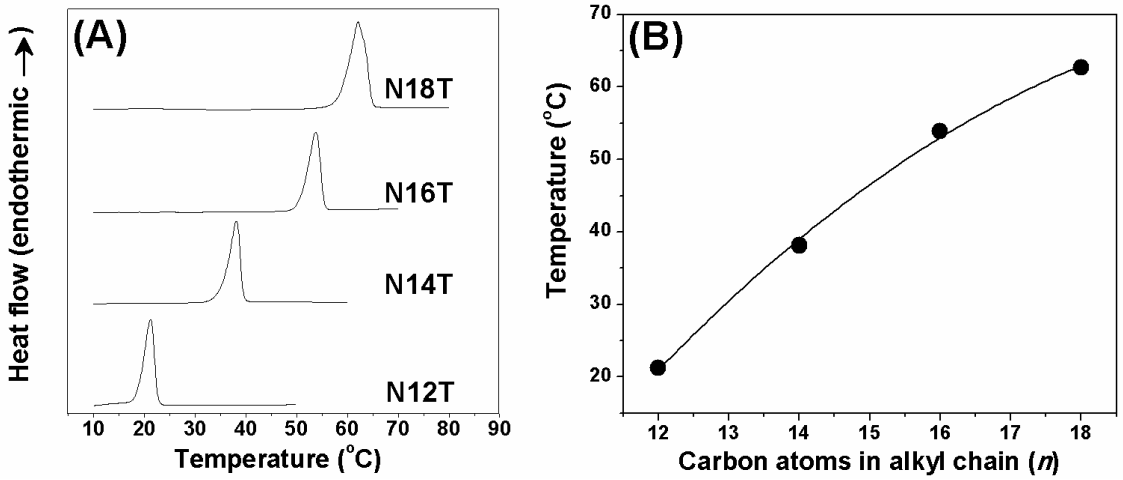

Figure 4: (A) DSC calorigrams of various N-acyl taurines and (B) Chain length dependence phase transition temperatures of NAT. Solutions were prepared in 10 mM phosphate buffer, pH -7.4.

Differential scanning calorimetric experiments were carried out to determine the phase transitions exhibited by the aqueous dispersions of NAT and to determine the change in enthalpy and change in entropy associated with the phase transitions. DSC heating scans of fully hydrated NAT were shown in Fig. 4A. Apart from *N*-decanoyltaurine, all other NATs showed broad transition with a full width at half maximum range between 2.6 to 3.8 ^{o}C. The transition temperatures of the NAT increases with increasing chain length though the magnitude of change decreases as the chain length increase (Fig. 4B). This is similar to the trends observed for the aqueous dispersion of fatty acids, *N*-acylethanolamines (NAE) [16], *N*-acyltyramine (NATA) [29], *N*-acyldopamines (NADA) [21], *N*-acylglycine (NAG) [19] and other *N*-acyl fatty acid amides [30]. A broad transition observed with NAT can be due to the coexistence of two phases over the temperature range before it proceeds to the complete fluid phase at high temperature. Similar broad transition was reported for palmitoylcarnitine, where it forms an interdigitated bilayer structure in gel phase and hexagonal phase (H_I) at high temperature [25]. However, further studies are required to delineate the exact structure of the NAT aggregates at different temperature.

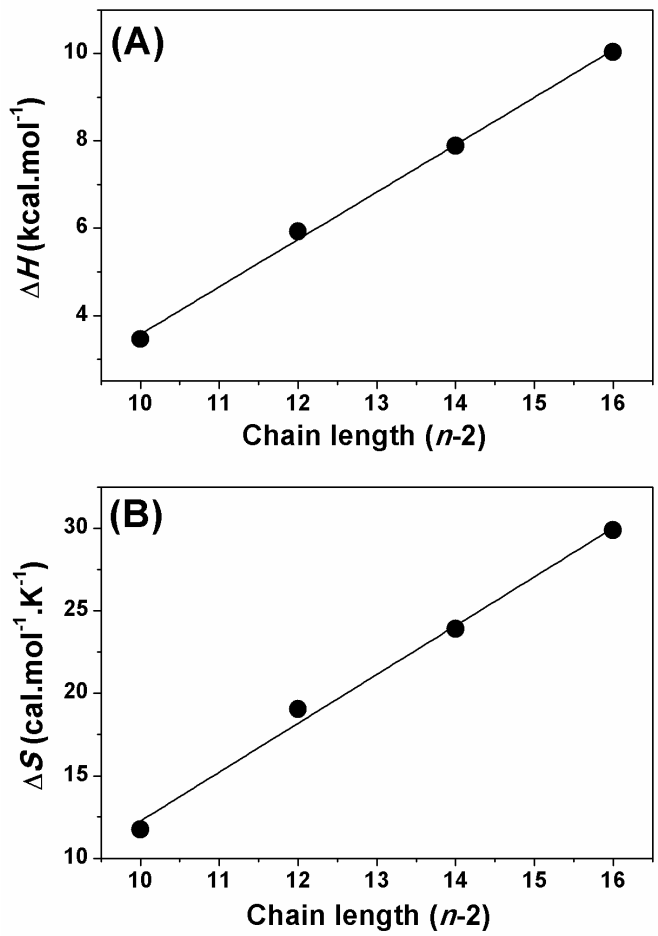

Figure 5: Chain length dependence of (A) transition enthalpies and (B) transition entropies of hydrated *N*-acyltaurines. Solid line represents linear least-squares fit of the data.

Table 3: Transition temperature (T_t), transition enthalpies (ΔH_t) and transition entropies (ΔS_t) of *N*-acyltaurines

acyl chain length	T_t (^oC)			ΔH_t (kcal.mol^{-1})	ΔS_t (cal.mol^{-1}.K^{-1})
	NAT				
12	21.24			3.46	11.76
14	38.13			5.92	19.02
16	53.89			7.89	23.90
18	62.65			10.04	28.88

The change in enthalpy and change in entropy associated with chain-melting phase transitions of various NAT are given in Table 3. Both transition enthalpy (ΔH_t) and transition entropy (ΔS_t) follows a linear trend with respect to chain length (n) and the data could be fitted with the following equation 2 and 3,

$$\Delta H_t = (n - 2)\, \Delta H_{inc} + \Delta H^0 \quad (2)$$

$$\Delta S_t = (n - 2)\, \Delta S_{inc} + \Delta S^0 \quad (3)$$

where ΔH^0 and ΔS^0 are the end contributions to the transition enthalpy and transition entropy, respectively, arising from the terminal methyl group and the polar head group region of NAT. ΔH_{inc} and ΔS_{inc} are the incremental values of transition enthalpy and transition entropy per methylene group. The linear chain length dependence of ΔH_t and ΔS_t indicate that the structure, molecular packing and intramolecular interaction of various NAT are likely to be very similar. From Fig. 5, the incremental values and end contributions of ΔH_t and ΔS_t were obtained from the linear least square analysis and presented in the Table 4.

Table 4: Incremental values (ΔH_{inc}, ΔS_{inc}) of chainlength dependence and end contributions (ΔH^0, ΔS^0) to phase transition enthalpy and entropy of *N*-acyltaurines.

Thermodynamic parameters	[a]NAE	NAT	[b]NAG
ΔH_{inc} (kcal.mol^{-1})	0.95	1.09 ± 0.03	1.15
ΔH^0 (kcal.mol^{-1})	-0.52	-7.28 ± 0.46	-4.34
ΔS_{inc} (cal.mol^{-1}.K^{-1})	2.37	2.96 ± 0.16	2.95
ΔS^0 (cal.mol^{-1}.K^{-1})	3.1	-17.36 ± 2.11	-10.06

[a]For comparison thermodynamic values are adopted from ref. [16]; [b]For comparison thermodynamic values are adopted from ref. [19]

As noted from Table 4, NAT displays larger negative end contributions of enthalpy, ΔH^0 and entropy, ΔS^0 than the NAEs and NAGs. The end contributions from enthalpy, ΔH^0 mainly arise from the taurine moiety. It was observed that upon hydration taurine moiety gains sustainable enthalpy stabilization (-7.28 ± 0.46 kcal.mol^{-1}) with the expense of ordering of water structure as a result reduction in entropy. The enthalpy stabilization could arise from hydrophobic and hydrogen bonding interactions. The negative ΔS^0 is also indicative of hydrophobic effect playing a role in the packing of NAT [21], which could arise due to the ordering of water molecules around the sulfonate moiety of the headgroup. ΔH_{inc} value of NAT was higher than NAEs [16] and comparable to NAGs [19], while ΔS_{inc} value of NAT was higher than NAEs and NAGs. These results indicated that the hydrophobic effect plays a role in the acyl chain packing of NAT, a similar observation was proposed for NAGs acyl chain packing. The average incremental contribution of each CH_2 to the transition enthalpy ΔH_{inc} and entropy, ΔS_{inc} is higher than NAE indicating a substantial contribution for NATs acyl chain packing comes from the repulsion between the charged head group. In addition to repulsion between headgroup at the interaface, the hydrogen bonding between the amide N-H and

carbonyl oxygen atoms of adjacent NAT molecules might contribute to high curvature in the head group region and resulted in higher ΔH_{inc} and ΔS_{inc}. NAT will not form micelles in the presence of NaCl, which supports the involvement of weak interaction such as H-bond in the stabilization of micelles (Fig. S15). Based on the thermodynamic analysis, we suggest that the hydrophobic forces govern the self-assembly of NATs acyl chains to form a hydrophobic core and expose the polar head group to the aqueous environment, as a result NATs prefer to adopt a micellar structure as characterized in the fluorescence study (Table 2).

4. Conclusion

A facile method to synthesize homologous series of NATs in reasonable yield with good purity was reported. The acyl chain length dependence of the CMC and phase transition exhibited by NATs has been investigated. The results obtained from fluorimetric titration indicate that the CMC follows a linear trend with respect to acyl chain length and obeys Trabue's rule. It has found that the energy of micellar formation of -0.61 kcal/mol per methylene group of the alkyl chain. The values of ΔH_{inc} andΔS_{inc} per CH_2 group of NATs is significantly higher than the NAEs, suggests the acyl chain packing differs considerably between NAEs and NATs. Moreover the higher negative end contributions of entropy, ΔS^0 and enthalpy, ΔH^0 observed with NATs indicate that the hydration of head group plays an important role in the self-assembly of NATs. Further studies aimed at the miscibility of NATs with other lipids, such as phosphatidylcholine and phophatidylethanolamine, is expected to offer detail insight into their biological role.

Acknowledgement

The Department of Science and Technology, Government of India (SB/FT/LS-217/2012) is acknowledged for the financial support. DST FIST grant to SCBT, SASTRA for establishing infrastructure facilities is gratefully acknowledged.

References

1. C. Ezzili, K. Otrubova, D. L. Boger, Fatty Acid Amide Signaling Molecules. Bioorg Med Chem Lett. 20 (2010) 5959–5968.
2. W.A. Devane, L. Hanus, A. Breuer, R.G. Pertwee, L.A. Stevenson, G. Griffin G, D. Gibson, A. Mandelbaum, A. Etinger, R. Mechoulam. Isolation and structure of a brain constituent that binds to the cannabinoid receptor. Science 258 (1992) 1946-1949.
3. H.A. Overton, A.J. Babbs, S.M. Doel, M.C.T. Fyfe, L.S. Gardner, G. Griffin, H.C. Jackson, M.J. Proctor, C.M. Rasamison, M. Tang-Christensen, P.S. Widdowson, G.M. Williams, C. Reynet. Deorphanization of a G protein-coupled receptor for oleoylethanolamide and its use in the discovery of small-molecule hypophagic agents. Cell Metab. 3 (2006) 167-175.
4. (a) K. Wakamatsu, T. Masaki, F. Itoh, K. Kondo, K. Sudo. Isolation of fatty acid amide as an angiogenic principle from bovine mesentery. Biochem. Biophys. Res. Commun. 168 (1990) 423-429. (b) A. Hamberger, G. Stenhagen, Erucamide as a modulator of water balance: new function of a fatty acid amide. Neurochem. Res. 28 (2003) 177-185.
5. (a) R. Succar, V.A. Mitchell, C.W. Vaughan. Actions of N-arachidonyl-glycine in a rat inflammatory pain model. Mol. Pain. 3 (2007) 24. (b) L.A.Q. Vuong, V.A. Mitchell, C.W. Vaughan, Actions of *N*-arachidonyl-glycine in a rat neuropathic pain model, Neuropharmacol. 54 (2008) 189-193.
6. H. Kozlowska, M. Baranowska, E. Schlicker, M. Kozlowski, J. Laudanski, B. Malinowska, Virodhamine relaxes the human pulmonary artery through the endothelial cannabinoid receptor and indirectly through a COX product. Br. J. Pharmacol. 115 (2008) 1034-1042.
7. K. K. Nichols, B. M. Ham, J. J. Nichols, C. Ziegler, K. B. Green-Church, Identification of Fatty Acids and Fatty Acid Amides in Human Meibomian Gland Secretions. Invest Ophthalmol Vis Sci. 48 (2007) 34-39.
8. A. Saghatelian, S.A. Trauger, E.J. Want, E.G. Hawkins, G. Siudzdak, B.F. Cravatt, Assignment of endogenous substrates to enzymes by global metabolic profiling. Biochemistry 43 (2004) 14332–14339.
9. A. Saghatelian, M.K. McKinney, M. Bandell, A. Patapoutian, B.F. Cravatt, A FAAH-regulated class of N-acyl taurines that activates TRP ion channels. Biochemistry 45 (2006) 9007–9015.
10. S.J. Reilly, E.M. O'Shea, U. Andersson, J. O'Byrne, S.E. Alexson, M.C. Hunt, A peroxisomal acyltransferase in mouse identifies a novel pathway for taurine conjugation of fatty acids, FASEB J. 21 (2007) 99–107.
11. J. O'Byrne, M.C. Hunt, D.K. Rai, M. Saeki, S.E. Alexson, The human bile acid-CoA:amino acid Nacyltransferase functions in conjugation of fatty acids to glycine, J. Biol. Chem. 278 (2003) 34237–34344.
12. J.Z. Long, M. LaCava, X. Jin, B.F. Cravatt, An anatomical and temporal portrait of physiological substrates for fatty acid amide hydrolase, J. Lipid Res. 52 (2011) 337–344.
13. M.K. McKinney, B.F. Cravatt, Structure-based design of a FAAH variant that discriminates between the N-acyl ethanolamine and taurine families of signaling lipids. Biochemistry 45 (2006) 9016-9022.

14. V. Chatzakos, K. Slätis, T. Djureinovic, T. Helleday, M.C. Hunt, N-Acyl taurines are antiproliferative in prostate cancer cells, Lipids 47 (2012) 355–361.
15. D. P. Waluk, K. Vielfort, S. Derakhshan, H. Aro, M. C. Hunt, N-Acyl taurines trigger insulin secretion by increasing calcium flux in pancreatic b-cells. Biochem. Biophys. Res. Comm. 430 (2013) 54–59.
16. M. Ramakrishnan, V. Sheeba, S.S. Komath, M.J. Swamy, Differential scanning calorimetric studies on the thermotropic phase transitions of dry and hydrated forms of *N*-acylethanolamines of even chainlengths, Biochim. Biophys. Acta, 1329 (1997) 302−310.
17. M.J. Swamy, P.K. Tarafdar, R.K. Kamlekar, Structure, phase behavior and membrane interactions of N-acylethanolamines andN-acylphosphatidylethanolamines, Chem. Phys. Lipids 163 (2010) 266–279.
18. B. Tan, D.K. O'Dell, Y.W. Yu, M.F. Monn, H.V. Hughes, S. Burstein, J.M. Walker. Identification of endogenous acyl amino acids based on a targeted lipidomics approach. , J Lipid Res. 51 (2010) 112-119.
19. S. Thirupathi Reddy, K. P. Krovi, M. J. Swamy, Structure and Thermotropic Phase Behavior of a Homologous Series of N‑Acylglycines: Neuroactive and Antinociceptive Constituents of Biomembranes. *Cryst. Growth Des.*, 14 (2014) 4944–4954
20. M. Connor, C.W. Vaughn, R.J. Vandenberg, N-Acyl amino acids and N-acyl neurotransmitter conjugates: neuromodulators and probes for new drug targets, Br. J. Pharmacol. 160 (2010) 1857–1871.
21. S.T. Reddy, P.K. Tarafdar, R.K. Kamlekar, M.J. Swamy, Structure and thermotropic phase behavior of a homologous series of bioactive N-acyldopamines, J. Phys. Chem. B 117 (2013) 8747–8757.
22. R. K. Kamlekar, M. J. Swamy, Studies on the Critical Micellar Concentration and Phase Transitions of Stearoylcarnitine, Biosci Rep. 26 (2006) 387–398.
23. V. V. de Souza, M. L. de Carvalho Noronha, F. L. Alves Almeida, C. A. Ribeiro Prado, A. C. Doriguetto, F. H. Florenzano, Cmc of PMMA-block-PDMAEMA measured vy NPN fluorescence, Polym. Bull. 67 (2011) 875-884.
24. D. Marsh, Handbook of Lipid Bilayers, CRC Press, Boca Raton, FL, 1990.
25. M.P. Veiga, M.A. Requero, F.M. Goni, A. Alonso, Effect of long-chain acyl-CoAs and acylcarnitines on gel–fluid and lamellar–hexagonal phospholipid phase transitions. Mol Membr Biol 13 (1996) 165–172
26. M.A. Requero, F.M. Goni, A. Alonso, The critical micellar concentrations of fatty acyl coenzyme A and fatty acyl carnitines. J Colloid Interface Sci 161 (1993) 343–346.
27. (a) H.J. Klevens, Structure and aggregation in dilate solution of surface active agents, J. Am. Oil Chem. Soc. 30 (1953) 74-80; (b) B. Kronberg, K. Holmberg, B. Lindman, Surface Chemistry of Surfactants and Polymers, Wiley-Blackwell, 2014.
28. M. Nakagaki, H. Komatsu, T. Handa. Estimation of critical micelle concentrations of lysolecithins with flurescent probes. Chem. Pharm. Bull. 34 (1986) 4479-4485.
29. S. Priscilla, D. Sivaramakrishna, V. Anbazhagan, Differential scanning calorimetric studies on the thermotropic phasebehavior of dry and hydrated forms of N-acyltyramines, Thermochimica Acta 586 (2014) 25–29
30. D. Marsh, M.J. Swamy, Derivatized lipids in membranes: physico-chemical aspects of N-biotinyl phosphatidylethanolamines,N-acylphosphatidylethanolamines and N-acylethanolamines, Chem. Phys.Lipids 105 (2000) 43–69.

Graphical abstract

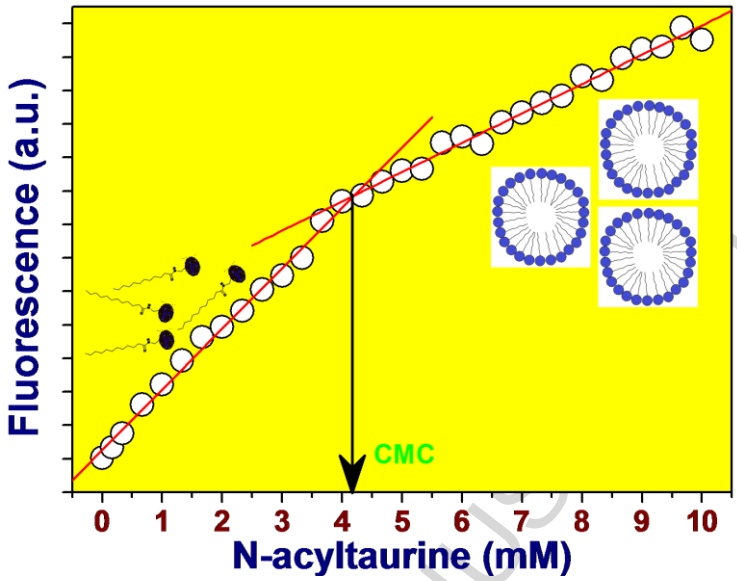

Highlights

- A simple procedure to synthesis of *N*-acyltaurine was reported
- NAT forms micelles, the CMC decreases with increasing alkyl chain length
- Phase transition temperature increases with increasing alkyl chain length
- Transition enthalpy and transition entropy follows linearity